Assessment of Reynolds Stress Turbulence Closures in the Calculation of a Transonic Separated Flow

Kwang-Yong Kim*, Jong-Woo Son, Chang-Ho Cho
School of Mechanical Engineering, Inha University, Inchon 402-751, Korea

In this study, the performances of various turbulence closure models are evaluated in the calculation of a transonic flow over axisymmetric bump. k-ε, explicit algebraic stress, and two Reynolds stress models, i. e., GL model proposed by Gibson & Launder and SSG model proposed by Speziale, Sarkar and Gatski, are chosen as turbulence closure models. SSG Reynolds stress model gives best predictions for pressure coefficients and the location of shock. The results with GL model also show quite accurate prediction of pressure coefficients downstream of shock wave. However, in the predictions of mean velocities and turbulent stresses, the results are not so satisfactory as in the prediction of pressure coefficients.

Key Words : Transonic Flow, Separation, Reynolds Stress Model, Axisymmetric Bump, Navier-Stokes Equations

1. Introduction

With the aid of rapid developments of computer technology and numerical algorithms, computational fluid dynamics (CFD) using the Reynolds-averaged Navier-Stokes equations has become a major tool for aerodynamic analysis of aircraft and turbomachinery. However, the development in turbulence modeling is rather slow. Furthermore, accuracy of the analysis is still limited by the performance of turbulence closure models.

The turbulence closure models have been developed from the simple mixing length models to the sophisticated second-moment closures during the past century. However, turbulence model with consistent accuracy and universality is not found, yet. Since most of turbulence closure models were tested for incompressible simple shear flows on their development stage, they have not been tested extensively for complex compressible flows, such as transonic flows with shock wave and separation. Thus, the performances of the models, especially, the second-order closures for transonic flows are not well known.

Shock-wave/boundary-layer interaction is an important phenomenon of flows in turbomachinery, and also of external flows over aircraft. The location and strength of the shock waves as well as the location of separation induced by shock-wave/boundary-layer interaction are essential factors to evaluate the aerodynamic performance in these applications. Therefore, accurate prediction of these phenomena is of practical importance.

Nietubicz, et al. (1980) obtained the numerical solution of thin-layer Navier-Stokes equations for transonic flows over axisymmetric slender body. This is regarded as a pioneering work which enables Navier-Stokes analysis for flows on transonic projectiles. A zero-equation model proposed by Baldwin and Lomax (1978) has been one of the most popular turbulence models in practical analysis of transonic flows, during the past two decades, mainly due to its simplicity. However, as Sahu and Danberg (1986) reported,

* Corresponding Author,
E-mail : kykim@inha.ac.kr
TEL : +82-32-872-3096 ; **FAX** : +82-32-868-1716
School of Mechanical Engineering, Inha University, 253 Yonghyun-Dong Nam-Gu Inchon 402-751 Korea.
(Manuscript **Received** August 17, 2000; **Revised** March 28, 2001)

this simple model, compared with k-ε model, had some problem in prediction for transonic flows. Bardina, et al. (1997) evaluated performances of three two-equation models (k-ω and k-ε models) and an one-equation model of Spalart and Allmaras (1992) for transonic flows. They concluded that the models were ranked with k-ω SST (Shear-Stress Transport) model proposed by Menter (1994) as the best overall model, followed by the Spalart and Allmaras one-equation model. On the other hand, Brakos and Drikakis (2000) examined the nonlinear two- and three-equation turbulence models for transonic flows over an axisymmetric bump. Their results showed that the nonlinear models improved the predictions in shock-wave/boundary-layer interaction, compared to the linear models. Abid, et al. (1995) used an explicit algebraic stress equation combined with k-ω and k-ε formulations to predict two-dimensional separated transonic flows, which gave some improvement over the standard two-equation models by taking account of nonequilibrium effects. A special version of second-moment closure, i. e., modified cubic Reynolds stress model was tested by Batten, et al. (1999) for several flows including complex compressible flows with shock-wave/boundary-layer interaction. To get the correct response to shock waves, they modified the Reynolds stress model of Craft and Launder (1996), which has been designed and tested with reference to both incompressible and compressible flows. From the results, it has been shown that the modified model gave better predictions than k-ω SST model in most of the test cases. As for the second-order closures, however, performances of well-known models such as proposed by Gibson and Launder (1987) and Speziale, et al. (1991), which have been most widely used in the calculations of incompressible flows, have not been reported for complex transonic flows, yet.

Among experimental works on transonic flows, Bachalo and Johnson (1986) investigated on turbulent boundary layer separation over an axisymmetric bump. They measured the mean velocity, turbulence intensity, and Reynolds shear stress profiles in the separated flow. The measurements of flowfield revealed that the flow was free from any three-dimensional effects and the interaction was relatively steady.

The aim of the present work is to evaluate the performance of two Reynolds stress models of Gibson and Launder (GL) (1987) and Speziale, Sarkar and Gatski (SSG) (1991), in comparison with those of algebraic stress model of Abid, et al. (1996) and standard k-ε model, in RANS (Reynolds-averaged Navier-Stokes equations) analysis of transonic flow over an axisymmetric bump, of which flowfield was measured by Bachalo and Johnson (1986).

2. Turbulence Closure Models

The Reynolds stress models employ the following mass-averaged transport equation for each stress component $(\overline{u_i u_j})$.

$$\frac{\partial(U_k\overline{u_i u_j})}{\partial x_k}=D_{ij}+P_{ij}+\Pi_{ij}-\varepsilon_{ij} \tag{1}$$

where D_{ij}, P_{ij}, Π_{ij}, and ε_{ij} represent diffusion, production, pressure-strain rate correlation, and dissipation terms, repectively.

$$D_{ij}=-\frac{\partial}{\partial x_k}(\overline{u_i u_j u_k})-\frac{1}{\rho}\left(\overline{\frac{\partial p u_j}{\partial x_i}}+\overline{\frac{\partial p u_i}{\partial x_j}}\right)+\nu\frac{\partial \overline{u_i u_j}}{\partial x_k x_k} \tag{2}$$

$$P_{ij}=-\left[\overline{u_j u_k}\frac{\partial U_i}{\partial x_k}+\overline{u_i u_k}\frac{\partial U_j}{\partial x_k}\right] \tag{3}$$

$$\Pi_{ij}=\frac{1}{\rho}\overline{\left[p\frac{\partial u_i}{\partial x_j}+p\frac{\partial u_j}{\partial x_i}\right]} \tag{4}$$

$$\varepsilon_{ij}=2\nu\overline{\frac{\partial u_i}{\partial x_k}\frac{\partial u_j}{\partial x_k}} \tag{5}$$

where U_i and u_i are mean and fluctuating velocity components, respectively. In this equation, D_{ij}, Π_{ij}, and ε_{ij} need to be modeled to close the equation. The simple gradient model of Daly and Harlow (1970) and the model based on local isotropy are used for turbulent diffusion and dissipation terms, respectively.

Models for the pressure-strain rate correlation term commonly have a general form as follows:

$$\Pi_{ij}=\alpha_1 kS_{ij}+\alpha_2 Pb_{ij}+\alpha_3 k\left(b_{ik}S_{ik}+b_{jk}S_{jk}-\frac{2}{3}\delta_{ij}b_{kl}S_{kl}\right)+\alpha_4 k\left(b_{ik}W_{jk}+b_{jk}W_{ik}\right) \tag{6}$$

Table 1 Pressure-strain model constants

	α_1	α_2	α_3	α_4
GL	0.8	0.	1.2	1.2
SSG	$0.8-1.3\ \Pi^{1/2}$	-1.8	1.25	1.40

where k and P are turbulent kinetic energy and its production rate, respectively. And, b_{ij}, S_{ij} and W_{ij} are anisotropy, strain rate and rotation tensors, respectively, defined by

$$b_{ij}=\frac{\overline{u_i u_j}}{2k}-\frac{1}{3}\delta_{ij} \tag{7}$$

$$S_{ij}=\frac{1}{2}\left(\frac{\partial U_i}{\partial x_j}+\frac{\partial U_j}{\partial x_i}\right) \tag{8}$$

$$W_{ij}=\frac{1}{2}\left(\frac{\partial U_i}{\partial x_j}-\frac{\partial U_j}{\partial x_i}\right) \tag{9}$$

The coefficients, in cases of GL and SSG models, are given in Table 1, where $\Pi=b_{lm}b_{ml}$ is a second-order invariant of anisotropy tensor. GL model employs additional wall reflection terms in the pressure-strain model (Gibson and Launder, 1987). The Reynolds stress models and standard k-ε model use an empirical wall function in near-wall regions.

The algebraic stress equation of Abid, et al. (1996) was derived based on the pressure-strain model of Speziale, et al. (SSG) (1991). The nonlinear constitutive equation of the model is solved in conjunction with the low-Reynolds-number equations for turbulent kinetic energy and its dissipation rate. Thus, in this model wall function is not employed.

The governing equations in generalized curvilinear coordinates for mean flow and turbulence are discretized by the finite volume method. For viscous and convection terms, central difference scheme and upwind scheme based on Roe's flux-difference splitting method are used, respectively.

As the boundary conditions, uniform velocities are assumed at the inlet, and zeroth order extrapolation, where the values at ghost points are obtained directly from the adjacent control volumes, is employed at the outlet.

3. Results and Discussion

Figure 1 shows a computational grid system for the transonic flow over an axisymmetric bump (Bachalo and Johnson, 1986). The longitudinal section of the bump is a circular arc, which has a 20.32 cm chord and a thickness of 1.905 cm. Its leading edge is joined to the cylinder by a smooth circular arc that is tangent to the cylinder and the bump at its two end points. The free stream Mach number is 0.875, and the total pressure and temperature are 95 kPa and 302 K, respectively. In the experiment (Bachalo and Johnson, 1986), a shock wave was generated of sufficient strength to produce a relatively large region of separated flow. Measurements were obtained by the laser velocimeter technique from upstream of separation through reattachment. Separation and reattachment locations were determined from oil-flow visualizations. 181×89 and 181×102 grid points were used in cases with and without wall function, respectively.

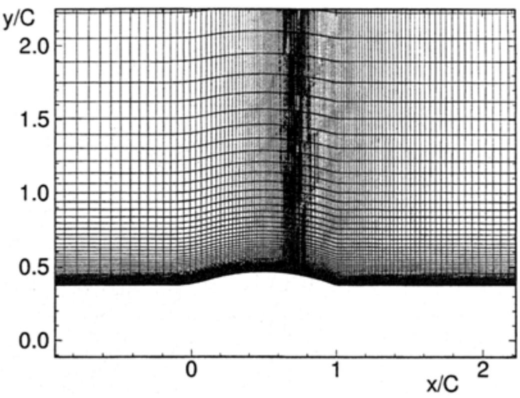

Fig. 1 Grid system

Measurements indicate that the shock wave takes place at 66 % chord downstream of leading edge of the bump. Table 2 shows predictions for the location of shock wave. In this case, SSG model gives the best result, and the algebraic stress model (Abid, et al., 1996) and GL model follow the next.

Shock-wave/boundary-layer interaction induces flow separation on the bump. In the experiment, the separation point at 4 % chord downstream of the shock wave, i. e., 70 % chord downstream of leading edge of the bump, and the reattachment point at 110 % chord downstream, were found. Thus, the length of the separation

Table 2 Locations of shock wave

Models	Exp.	k-ε	Algebraic stress	GL	SSG
Location (% of chord)	66.0	70.7	68.9	69.1	65.7

Table 3 Separation and reattachment points

Models	Exp.	k-ε	Algebraic stress	GL	SSG
Separation point (% of chord)	70.0	74.8	68.9	74.6	73.7
Reattachment (% of chord)	110.0	109.8	111.3	109.6	110.8

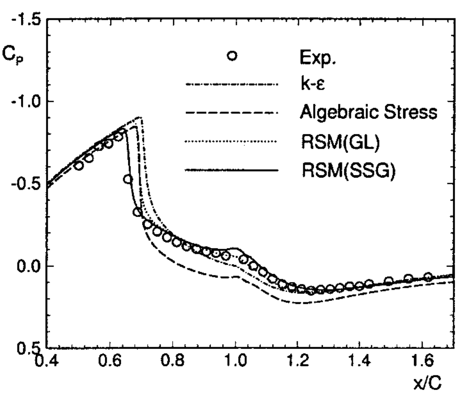

Fig. 2 Possure coefficients

bubble was 40 % chord. Table 3 shows predictions for the separation and reattachment points. The separation point and the length of the separation bubble are best predicted by the algebraic stress model. However, it is noted that the separation coincides with the shock wave. All of the remaining models, i. e., two Reynolds stress models and standard k-ε model, commonly predict the late separation and the smaller separation bubble.

Figure 2 compares the computational results of pressure coefficient with four different turbulence models. SSG model gives the results which show best agreement with experimental distribution. The results with GL model also show good agreement except location of the shock wave. But, the algebraic stress model predicts considerably smaller values of pressure coefficient downstream of the shock wave.

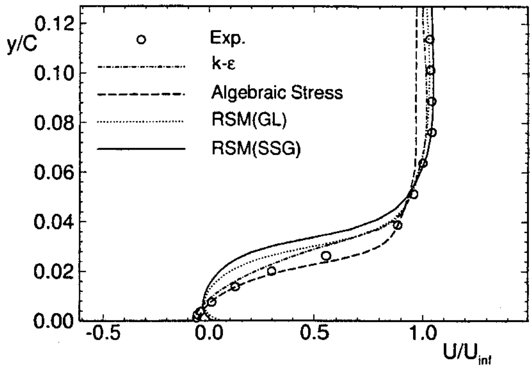

Fig. 3 Mean axial velocity profiles at 87.5 % chord

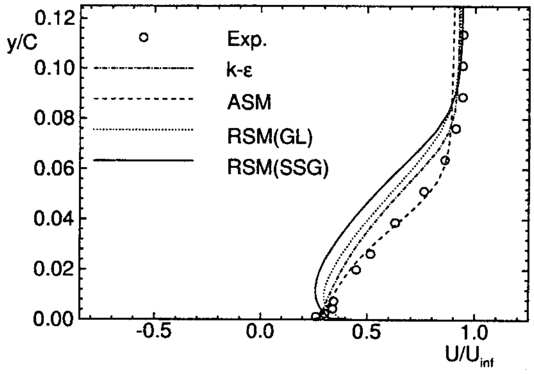

Fig. 4 Mean axial velocity profiles at 125 % chord

Figures 3 and 4 show mean axial velocity profiles at 87.5% and 125% chord locations, in the separation region and downstream of the reattachment point, respectively. Unlike the prediction for pressure coefficient (Fig. 2), algebraic stress model produces the best results. The results with the Reynolds stress models commonly show velocity peak just adjacent to the wall at 125% chord location. As the results with low-Reynolds -number Reynolds stress model of Batten, et al. (1999) showed less remarkable, but similar trend, the rate of flow recovery following reattachment is generally underestimated by current second -order closures. Thus, the discrepancies in the mean velocity profiles are not fully attributed to the logarithmic wall function which is not valid in a separation region.

The Reynolds stress models were expected to show the better performance, especially in the prediction of turbulence quantities, than lower order closure models, which did not take account

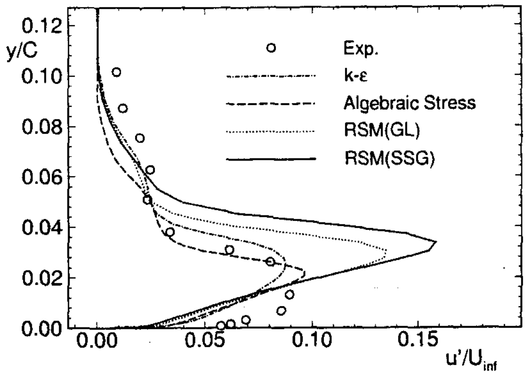

Fig. 5 Turbulent intensity profiles at 87.5 % chord

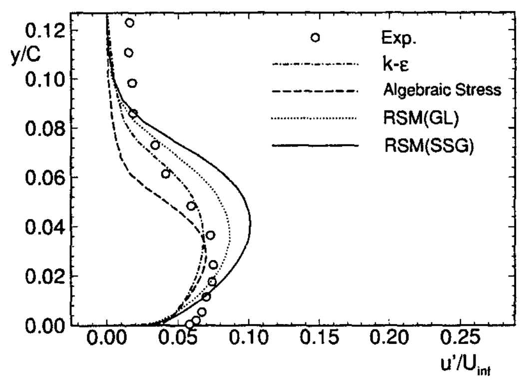

Fig. 6 Turbulent intensity profiles at 125 % chord

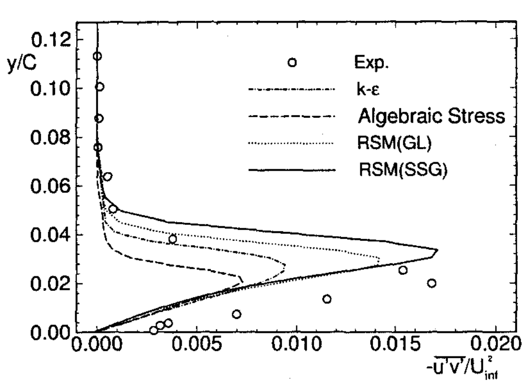

Fig. 7 Turbulent shear stress profiles at 87.5 % chord

of the effects of extra strain rates. However, in this test case, the Reynolds stress models fail to predict correct level of turbulent normal stress as in Figs. 5 and 6, where both algebraic stress and k-ε models produce rather resonable profiles. While SSG model successfully predicts the peak level of shear stress (Figs. 7 and 8), the locations of peak value are shifted considerably outward.

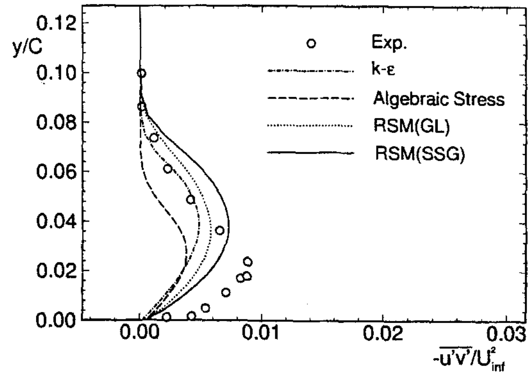

Fig. 8 Turbulent shear stress profiles at 125 % chord

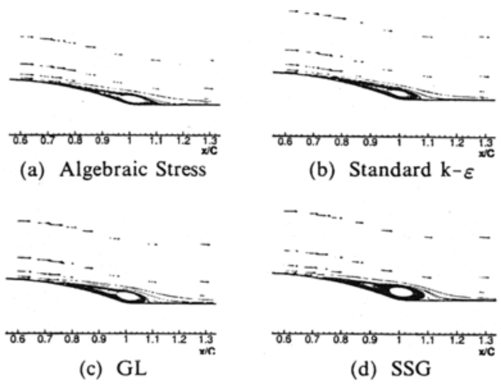

Fig. 9 Velocity vectors and streamlines

Figure 9 shows the streamlines and velocity vectors around the separation region. As can be deduced from the mean velocity profiles, the SSG model predicts the thickest region, while the algebraic stress model predicts the longest.

In the calculation of the other types of transonic flow including a three-dimensional flow (Cho and Kim, 2001), the similar performances of the turbulence models are also found.

The amounts of computing time that are required to converge the solutions with algebraic stress, GL and SSG models are approximately 1.4, 4.2 and 4.5 times the computing time with k-ε model, respectively.

4. Conclusion

Performances of two Reynolds stress models of Gibson and Launder (GL) and Speziale, Sarkar and Gatski (SSG), were evaluated in comparison with those of an algebraic stress model and standard k-ε model, in the analysis of a transonic flow over an axisymmetric bump. SSG model shows the best overall performance in predictions for pressure coefficients and location of shock. However, in the predictions for mean velocities and turbulent intensity, the algebraic stress model without empirical wall function, rather than the Reynolds stress models, gives best agreement with experimental profiles. Flow recovery downstream of the reattachment is quite delayed by the Reynolds stress models. The low-Reynolds-number expansion of the second order closures is expected to improve the results. But, concerning the essential problem of delayed flow recovery, further researches on the second order modeling are required.

References

Abid, R, Morrison, J. H., Gatski, T. B, and Speziale, C. G., 1996, "Prediction of Aerodynamic Flow with a New Explicit Algebraic Stress Model," *AIAA Journal*, Vol. 34, No. 12, pp. 2632～2635.

Abid, R., Rumsey, C., and Gatski, T. B., 1995, "Prediction of Nonequilibrium Turbulence Flows with Explicit Algebraic Stress Models," *AIAA Journal*, Vol. 33, No. 11, pp. 2026～2031.

Bachalo, W. D., and Johnson, D. A., 1986, "Transonic, Turbulent Boundary-Layer Separation Generated on an Axisymmetric Flow Model," *AIAA Journal*, Vol. 24, No. 3, pp. 437～443.

Baldwin, B. S., and Lomax, H., 1978, "Thin Layer Approximation and Algebraic Model for Separated Turbulent Flows," *AIAA Paper* 78-257.

Barakos, G., and Dirkakis, D., 2000, "Investigation of Nonlinear Eddy-Viscosity Turbulence Models in Shock/Boundary-Layer Interaction," *AIAA Journal*, Vol. 38, No. 3, pp. 461～469.

Bardina, J. E., Huang, P. G., and Coakley, T. J., 1997, "Turbulence Modeling Validation," *AIAA Paper* 97-2121.

Batten, P., Craft, T. J., Leschziner, M. A., 1999, "Reynolds-Stress- Transport Modeling for Compressible Aerodynamics Applications," *AIAA Journal*, Vol. 37, No. 7, pp. 785～797.

Cho, C. H., and Kim, K. Y., 2001, "Evaluation of Turbulence Closure Models in the Calculation of Transonic Flow," submitted to *Journal of KSAS*.

Craft, T. J., and Launder, B. E., 1996, "A Reynolds Stress Closure Designed for Complex Geometries," *International Journal of Heat and Fluid Flow*, Vol. 17, No. 3, pp. 245～254.

Daly, B. J. and Harlow, F. H., 1970, "Transport Equations in Turbulence," *Physics of Fluids*, Vol. 13, pp. 2634～2649.

Gibson, M. M., and Launder, B. E., 1987, "Ground Effects on Pressure Fluctuations in the Atmospheric Boundary Layer," *Journal of Fluid Mechanics*, Vol. 86, No. 3, pp. 491～511.

Menter, 1994, "Two-Equation Eddy-Viscosity Turbulence Models for Engineering Applications," *AIAA Journal*, Vol. 32, No. 8, pp. 1598～1605.

Nietubicz, C. J., Pulliam, T. H., and Steger, J. L., 1980, "Numerical Solution of the Azimuthal-Invariant Thin-Layer Navier-Stokes Equations," *AIAA Journal*, Vol. 18, pp. 1411～1412.

Sahu, J., and Danberg, J. E., 1986, "Navier-Stokes Computations of Transonic Flows with a Two-Equation Turbulence Model," *AIAA Journal*, Vol. 24, No. 11, pp. 1744～1751.

Sparart, P. R., and Allmaras, S. R., 1992, "A One-Equation Turbulence Model for Aerodynamic Flows," *AIAA Paper* 92-0439.

Speziale, C. G., Sarkar, S., and Gatski, T. B., 1991, "Modelling the Pressure-Strain Correlation of Turbulence: An Invariant Dynamics Approach," *Journal of Fluid Mechanics*, Vol. 227, pp. 245～272.